



Targeted Adaptive Chaos Control of Regimes and Eddy Strength in Two Lorenz Models

Moyan Liu¹, Qin Huang¹, Upmanu Lall^{1,2}

¹School of Complex Adaptive Systems & Water Institute, Arizona State University, Tempe, AZ, 85281, USA.

5 ²Department of Earth and Environmental Engineering & Columbia Water Center, Columbia University, New York, 10025, NY, USA.

Correspondence to: Upmanu Lall (ulall@asu.edu)

Abstract. Extreme weather events present growing challenges as climate changes. “Weather Jiu-Jitsu” is a proposal to nudge atmospheric circulation to redirect or defuse these extreme events by leveraging the sensitivity of chaotic atmospheric dynamics to initial conditions. We demonstrate an optimal control strategy to stabilize two low-order models of atmospheric dynamics, the Lorenz 63 (L63) and Lorenz 84 (L84). Estimated local Lyapunov exponents (LLE) are used to decide when to apply control. In L63, regime transitions are treated as model analogs of persistent circulation states of concern, while in L84, large eddy amplitudes serve as conceptual surrogates for synoptic-scale moisture transport events such as atmospheric rivers. The timing and amplitude of nudges is solved over a forecast horizon to minimize the total energy applied, while ensuring that the trajectory remains within predefined bounds to avert undesirable consequences. We explicitly incorporate multiplicative noise, randomly selecting a trajectory from an ensemble forecast to apply control, thus reflecting the mismatch between model and reality that would arise in operational applications.

1 Introduction

Climate change is intensifying extreme events such as droughts, floods, heat waves, and freezes, causing severe global socio-economic impacts (Robinson et al., 2021). These effects are further exacerbated by growing populations and increasing economic activity (Mario et al., 2024). While current strategies or policies such as decarbonization and the energy transition can reduce greenhouse gas emissions, they do not directly mitigate the immediate risks posed by extreme weather events (Zhao, 2025). Approaches like weather modification and geoengineering require vast amounts of energy and are hindered by significant technical and ethical concerns (Sugiyama et al., 2025; Yeh, 2025). Meanwhile, scaling aging and inadequate physical, financial, and social infrastructure to enhance resilience remains a formidable challenge (Hwang and Lall, 2024). These challenges are complicated by the difficulty in predicting the underlying atmospheric processes that drive extreme weather, particularly persistent atmospheric blocking patterns associated with anomalous jet stream behaviour and synoptic scale eddies in the mid-latitudes (Nabizadeh et al., 2019; Han and Singh, 2021; Aemisegger et al., 2021; Kim et al., 2024).

We propose an initiative (Huang et al., 2025) we call “Weather Jiu-Jitsu” to mitigate weather extremes by defusing or redirecting atmospheric circulation trajectories using recurrent nudging with small perturbations that leverages the



underlying nonlinear dynamics to amplify the effect of the nudges. For our purposes, we view Lorenz 63 model regime shifts as conceptual analogs of persistent circulation anomalies, while in Lorenz 84 model we associate high eddy amplitudes with surrogates of synoptic-scale features such as atmospheric rivers. These are not meteorological extremes, but they provide testbeds for asking whether such states can be suppressed or redirected in a controlled setting. This differs from prior chaos control studies, which typically focused on trajectory stabilization without reference to physically motivated extreme states.

The Lorenz 63 (L63) model, emerged from a collaboration between Edward Lorenz and Barry Saltzman and is a notable conceptual example in chaos theory and atmospheric dynamics (Saltzman, 1959; Lorenz, 1963; Saltzman, 1957). L63 exhibits sensitive dependence to initial conditions, and given the shape of its attractor, it led to the well-known expression “butterfly effect” (Lorenz, 1963; Glasner and Weiss, 1993).

The Lorenz 84 (L84) model represents mid-latitude atmospheric circulation under external forcing by the equator to pole temperature gradient and land ocean temperature contrast. The forcing can consider seasonal variability and El Nino Southern Oscillation (ENSO) dynamics (Lorenz, 1984; Broer et al., 2002; Karamperidou et al., 2012). It captures certain features of atmospheric behaviour that underlie extreme weather, including jet stream oscillations and eddy dynamics (Madonna et al., 2017; Lorenz, 1990; Faranda et al., 2019). These models serve as conceptual testbeds for understanding how weather and climate system can shift into hazardous states and how targeted interventions might delay or deflect such shifts (Palmer, 2006; Macmynowski, 2010; Shen et al., 2021; Saiki and Yorke, 2023).

Chaos control techniques have been applied across various fields, including weather and climate systems (Hoffman, 2002; Miyoshi and Sun, 2022). For example, Control Simulation Experiments (CSE) and Model Predictive Control (MPC), coupled with data assimilation, have been developed to keep the L63 system confined to one wing of the butterfly attractor with control and optimization algorithms, demonstrating successful control outcomes (Ogorzałek, 1994; Ouyang et al., 2023; Kawasaki and Kotsuki, 2024; Nagai et al., 2024; Mitsui et al., 2025). One of the first methods is the Ott-Grebogi-Yorke (OGY) method, which stabilizes chaotic trajectories by applying small perturbations to system parameters when the system naturally approaches an unstable periodic orbit embedded within the chaotic attractor (Ott et al., 1990; Grebogi and Lai, 1997). Adaptive targeting methods guide chaotic systems toward desired states using observed trajectories and feedback perturbations (Boccaletti et al., 1997; Bollt, 2003). Time-delayed Feedback Control stabilizes unstable periodic behaviour by applying a correction based on the difference between the system’s current state and its own state at a previous time (Pyragas and Pyragas, 2006; Postlethwaite and Silber, 2007; Purewal et al., 2016; Ding and Lei, 2023). Sliding Mode Control approach has also been applied to the L63 model. It forces the system’s state to reach and stay on a predefined surface in the state space (Yu, 1996; Yang et al., 2002; Yau and Yan, 2004).

The past work signals the potential for ‘Weather Jiu-Jitsu’. Here, we benchmark an approach that considers an ensemble of trajectory evolution, and the role of “dynamical” noise and thus account for stochastic aspects. These



considerations allow a more realistic assessment of an adaptive control strategy than has been done in prior work on idealized models. Instead of applying persistent interventions at every time step, we introduce a method that activates control only when a potential regime shift is detected, using real-time evaluation of the stability of the state space, as measured by local Lyapunov exponents (LLE) (Eckhardt and Yao, 1993; Guégan and Leroux, 2009). Once triggered by a LLE that exceeds a specified threshold, we solve a constrained optimization problem over a specified forecast horizon, to solve for minimal energy perturbations required to direct the system into a desired regime. The strategy is implemented and then re-evaluated at each forward time step, randomly choosing a trajectory from the ensemble generated upon implementation. This approach not only ensures efficient use of control energy resources but also enhances realism by respecting physical limits and maintaining the system's inherent variability.

2 Methods

Our approach is developed and demonstrated on both Lorenz models, though with slightly different objectives. With the L63 model, we consider a goal to keep the trajectories confined to one wing of the butterfly, representing regime control. The intention was to show that our approach is effective, even in the presence of noise. With the L84 model, we consider that strong eddies would represent potentially extreme tropical moisture exports or atmospheric rivers and seek to limit their amplitude by perturbation. This is a more complex forced system, and this experiment gets a little closer to the idea of controlling weather extremes in an idealized environment.

2.1 Lorenz Systems

The Lorenz 1963 (L63) model (Lorenz, 1963) was originally developed to represent atmospheric convection and comprises the following three equations:

$$\frac{dx}{dt} = \sigma(y - x), \quad (1)$$

$$\frac{dy}{dt} = x(\rho - z) - y \quad (2)$$

$$\frac{dz}{dt} = xy - \beta z, \quad (3)$$

Here, x corresponds to the intensity of convective motion, while y and z represent horizontal and vertical temperature differences. The parameters σ , ρ , and β govern the strength of coupling and dissipative processes. The system exhibits a distinctive butterfly-shaped attractor, with trajectories chaotically switching between two "wings," each corresponding to quasi-stable atmospheric regimes. These regime switches iconify transitions between different climate or weather patterns. The L63 model is widely used in chaos control research, allowing benchmarking of control strategies.

We consider the two wings of the attractor as two climate regimes and implement a control strategy that steers the system's trajectory toward one desired regime. This represents a form of anticipatory intervention to avoid undesirable futures, such as the onset of extreme weather scenarios. The L63 trajectories are simulated with a fourth-order Runge-



Kutta scheme with a fixed time step of $\Delta t=0.01$, and standard parameter values ($\sigma = 10.0$, $\rho = 28.0$, $\beta = 8/3$). For the initial experiment, the initial state [8.20747939, 10.0860429, 23.86324441] is taken from a previous paper (Miyoshi and Sun, 2022), which is selected for its relatively stable behaviour at early stages. We constrain the active state space to be $(x, y, z) \in [(0, 10), (0, 20), (0, 30)]$. For each experiment, we consider a total evolution of 2000 time steps from the initial condition.

The Lorenz 1984 (L84) model is a truncated representation of large-scale atmospheric dynamics at mid-latitudes (Lorenz, 1984; Van Veen, 2003; Freire et al., 2008), with the dynamics defined by the following sets of ordinary differential equations.

$$\frac{dX}{dt} = -Y^2 - Z^2 - aX + aF, \quad (4)$$

$$\frac{dY}{dt} = XY - bXZ - Y + G \quad (5)$$

$$\frac{dZ}{dt} = bXY + XZ - Z, \quad (6)$$

Here, X represents the strength of the zonal jet stream, Y and Z describe the amplitudes of the cosine and sine phases of eddies. Nonlinear interaction terms (XY , XZ) represent the amplification of eddies through energy exchange with the jet stream, while $-Y^2$ and $-Z^2$ in the X -equation indicate energy loss from the jet due to this amplification. The terms $-bXZ$ and bXY represent the advection or displacement of the eddies by the mean flow, with $b > 1$ implying faster displacement than amplification. Linear damping terms reflect mechanical and thermal dissipation, with time scaled so that the eddy damping rate is unity and the zonal flow damping rate is scaled by a factor $a < 1$. This non-autonomous model includes two external forcing parameters: the equator to pole temperature gradient (F), and the land-ocean temperature contrast (G). These can be allowed to vary in time to represent seasonality of forcing, and can also be coupled to ENSO models to reflect the atmospheric forcing due to different ENSO phases (Karamperidou et al., 2012). In the present work, we considered them to be particular seasonal condition.

Synoptic and low-frequency eddies are the primary drivers of ocean-to-land moisture transport in the extratropics with Atmospheric Rivers (ARs) representing concentrated channels of such transport largely formed by synoptic eddies (Zhu and Newell, 1998; Newman et al., 2012). Motivated by this, we implement a control strategy in the L84 model by constraining the combined eddy amplitude, measured as the sum of the absolute values of Y and Z to remain below a prescribed threshold, as described in Section 3.4. This approach aims to mimic the suppression of excessive eddy activity that may lead to ARs. The L84 trajectories are also simulated with a fourth-order Runge-Kutta scheme with a fixed time step of $\Delta t=0.01$, employing standard parameter values ($F=8.0$, $a=0.25$, $b=4.0$, $G=1.0$).

2.2 Local Lyapunov Exponents

The solution space of Lorenz models can be considered as a nonlinear dynamical map, where the future state depends in a complex and sensitive way on the current one. We develop a surrogate dynamical map to approximate both the L63 and L84 dynamics (see Supporting Information S1).



Forecasts of chaotic systems are characterized by the exponential divergence of nearby trajectories. The rate of this divergence is quantified by the Lyapunov Exponent (LE) (Liapounoff, 1907; Wolf et al., 1985). A positive LE indicates that nearby trajectories will diverge with time, while 0 or negative values reflect stability. We focus on the local Lyapunov exponent (LLE), which evaluates divergence rates over short time intervals and localized regions of the state space, enabling the detection of transient instability and regime shifts in real time (Eckhardt and Yao, 1993; Guégan and Leroux, 2009). If the LLE is positive an appropriately placed perturbation may amplify in the desired direction, while if the LLE is 0 or negative, changing the trajectory by perturbation may require substantial energy input. Further, in the positive LLE situation, even after perturbation the trajectories are wont to diverge so tracking the actual trajectory that emerges over an operational forecast and control horizon and refocusing it becomes necessary.

Metrics such as the finite-size Lyapunov exponent (FSLE) and finite-time Lyapunov exponent (FTLE) have been developed to quantify predictability over spatial scales or finite durations respectively (Lapeyre, 2002; Aurell et al., 1997). These would be useful once we consider spatially extended systems.

To assess local instability, we compute the LLE using the Jacobian matrix of the surrogate system represented by the map. For a dynamical system of the form $\dot{x} = f(x(t))$, where $x \in \mathbb{R}^n$ is the state vector and f is a nonlinear vector field, the Jacobian matrix $J(x)$ is defined as:

$$J(x) = \frac{\partial f}{\partial x} = \begin{bmatrix} \frac{\partial f_1}{\partial x_1} & \dots & \frac{\partial f_1}{\partial x_n} \\ \vdots & \ddots & \vdots \\ \frac{\partial f_n}{\partial x_1} & \dots & \frac{\partial f_n}{\partial x_n} \end{bmatrix} \quad (7)$$

To detect instability, we compute the largest real part of the eigenvalues of the Jacobian as LLE:

$$\lambda(x) = \max(\Re(\text{eigvals}(J(x)))) \quad (8)$$

2.3 Experiment Design

The overall workflow (Figure 1) follows a structured pipeline consisting of state evolution, instability detection, control optimization, and performance assessment.

We first calculate the LLE of the current state. If the LLE remains below a prescribed threshold, no control is exercised. If the LLE goes above the threshold, the control mechanism is triggered. We generate 50 ensemble members adding Gaussian noise, in order to account for uncertainty in both the system evolution and model predictions. From this ensemble, one member is randomly selected as the control target, and the optimization algorithm for control is applied to it. The optimization seeks to minimize the total energy used for control by selecting a bounded perturbation sequence. The trajectory is evolved using the sequence, with a random member of the ensemble picked at every time step, and the LLE criteria checked at every step to decide if the optimization should be performed again.



170

The white noise amplitude is proportional to the output of the map as the current state, to account for model imperfections and observational uncertainty. Before applying the control, the resulting trajectory is re-evaluated over a short verification horizon. If the trajectory remains within the specified bounds, the control is accepted and applied. If not, the optimization is repeated up to a maximum number of attempts. If no successful control is found, the one with the lowest cumulative constraint violation is applied as a fallback.

175

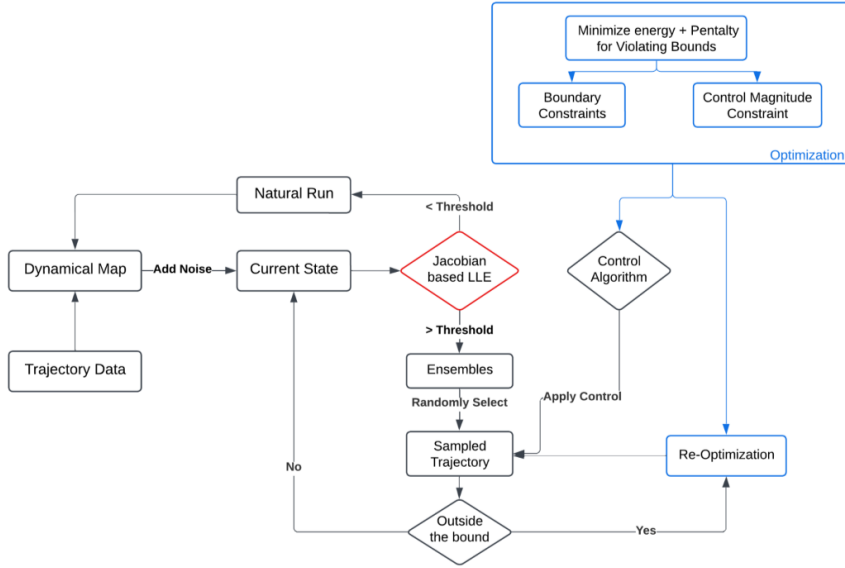


Figure 1: Workflow of Control Framework

The perturbation is quantified by u_t , and the control energy is defined as u_t^2 . For performance assessment, we compute the ratio of control energy to total system energy at each time step. This ratio is given by:

$$\frac{E_{control}}{E_{total}} = \frac{dx^2 + dy^2 + dz^2}{X^2 + Y^2 + Z^2} \quad (9)$$

where (dx, dy, dz) represents the control perturbation vector, and (X, Y, Z) is the system state at the moment of control application. This metric allows us to evaluate the efficiency and subtlety of the intervention.

2.4 Optimized Control on Triggering

The control objective is to minimize the total energy applied via perturbations over the control horizon (typically specified as 10 time steps). The decision variables are the magnitude of the state perturbations calculated as the Euclidean norm of the perturbation vector at time t .

$$\min_{\delta X_t} \sum_{t=1}^T (u_t^2 + \lambda \sum_{j=1}^3 \text{penalty}_{t,j}(X_t)) \quad (10)$$

$$u_t = \|\delta X_t\|_2, \quad t = 1, \dots, T \quad (11)$$



For each time step over the control horizon, a random noise term is injected into the model dynamics with the magnitude of m . To maintain feasibility, the magnitude of the control input is also constrained by a maximum allowable perturbation magnitude D_{max} to prevent unrealistically large perturbations.

$$X_t = f(X_{t-1}) + \varepsilon_t, \quad \varepsilon_t \sim N(0, m \cdot |X_{t-1}|) \quad (12)$$

$$u_t \leq D_{max}, \quad t = 1, \dots, T \quad (13)$$

The resulting trajectory is required to lie within prescribed bounds to effect control. A penalty is added for each component of the forecasted state that violates its respective safety range, defined by lower and upper limits, l_j and h_j . The penalty weight λ governs the trade-off between minimizing control effort and enforcing state constraints.

$$penalty_{t,j} = \begin{cases} l_j - x_{t,j}, & \text{if } x_{t,j} < l_j \\ x_{t,j} - h_j, & \text{if } x_{t,j} > h_j \\ 0, & \text{otherwise} \end{cases} \quad (14)$$

This model is solved using the Sequential Least Squares Programming (SLSQP) optimization algorithm (Kraft, 1988). If needed, the re-optimization is executed up to 8 times at a particular time step..

We do not consider data assimilation, but track the actual evolution of the system by randomly sampling a trajectory from the potential ensemble at each time step, and re-initiating the process from that condition. We have considered a chance constrained or probabilistic constraint set as an alternative, but decided to use the approach presented here since it allows us to directly mimic what may happen under sequential application of a strategy in practice.

3 Results

We present the application of the schema from the previous section to the L63 and L84 experiments.

3.1 Control of L63 Effectively Suppresses Regime Transitions

The proposed control framework confines the L63 trajectory to one wing of the attractor, eliminating transitions between regimes. In the uncontrolled simulation, the system frequently switches between the two wings of the Lorenz attractor, reflecting the inherent chaotic nature of the model. When the control strategy is applied, these transitions are suppressed, and the trajectory remains on a single wing for the duration of the 2000-step simulation (Figure 2 (a, b) and Supporting Information S3). Control interventions were triggered at only 201 time steps, with most perturbation magnitudes below 0.5. The control energy, measured as a percentage of total system energy, remained under 0.03% in nearly all cases (Figure 2 (c, d)). These results highlight the controller's ability to maintain the system in a stable regime using minimal and optimized interventions.

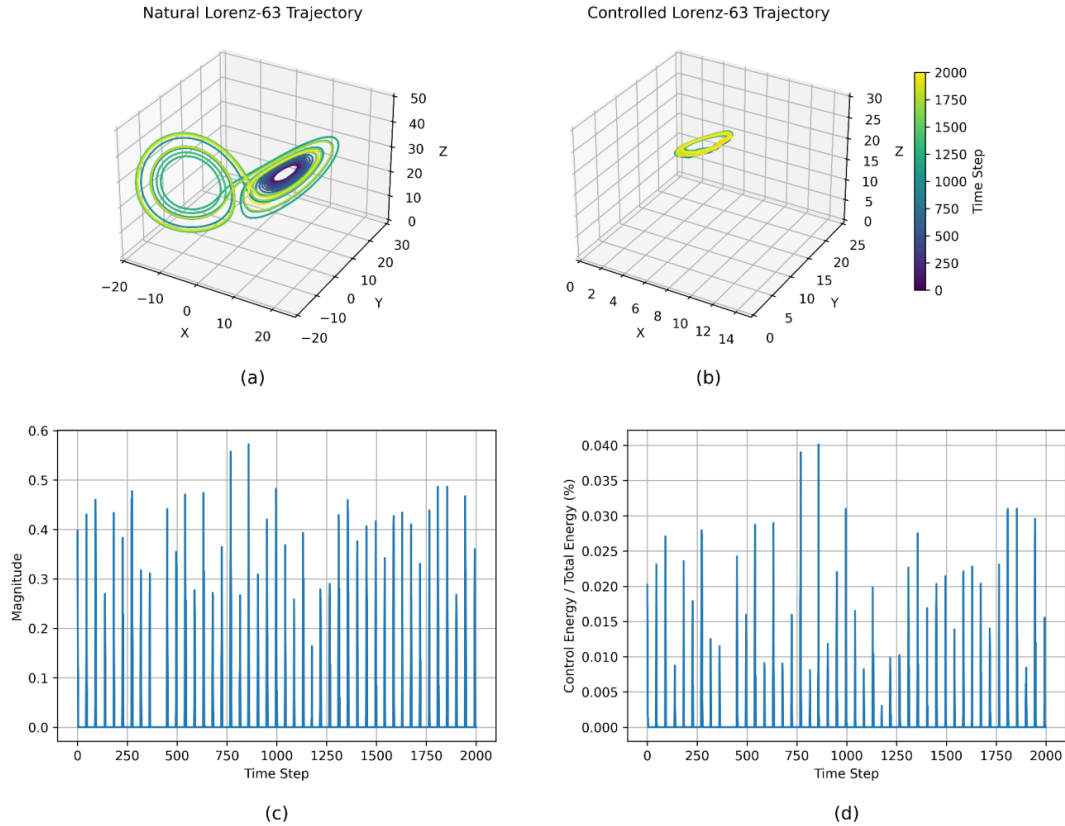


Figure 2: Comparison of natural (a) and controlled (b) L63 trajectories. (c) shows the magnitude of perturbations applied at each step, and (d) displays the ratio of control energy to total system energy over time.

3.2 Infeasible Control Given Initial Condition Scenario

220 The initial state $[1, 1, 1]$ lies near the boundary separating the two wings of the L63 attractor wings, a location known to be highly sensitive to perturbations. In this case, the natural trajectory exhibits rapid transitions between regimes, making stabilization difficult (Figure 3). The controller struggles to suppress this instability due to the constraint on maximum allowable perturbation. Control was triggered 214 times (compared to 201 in the baseline), with early perturbations often exceeding a magnitude of 1.0. The energy input also rose with control energy exceeding 0.5% of

225 total system energy in the early time steps. However, once the system settled near one wing, both the magnitude and frequency of interventions decreased substantially. This behaviour illustrates the importance of an early state selection for intervention, since it is difficult to intervene close to regime transitions where the LLEs are very high.

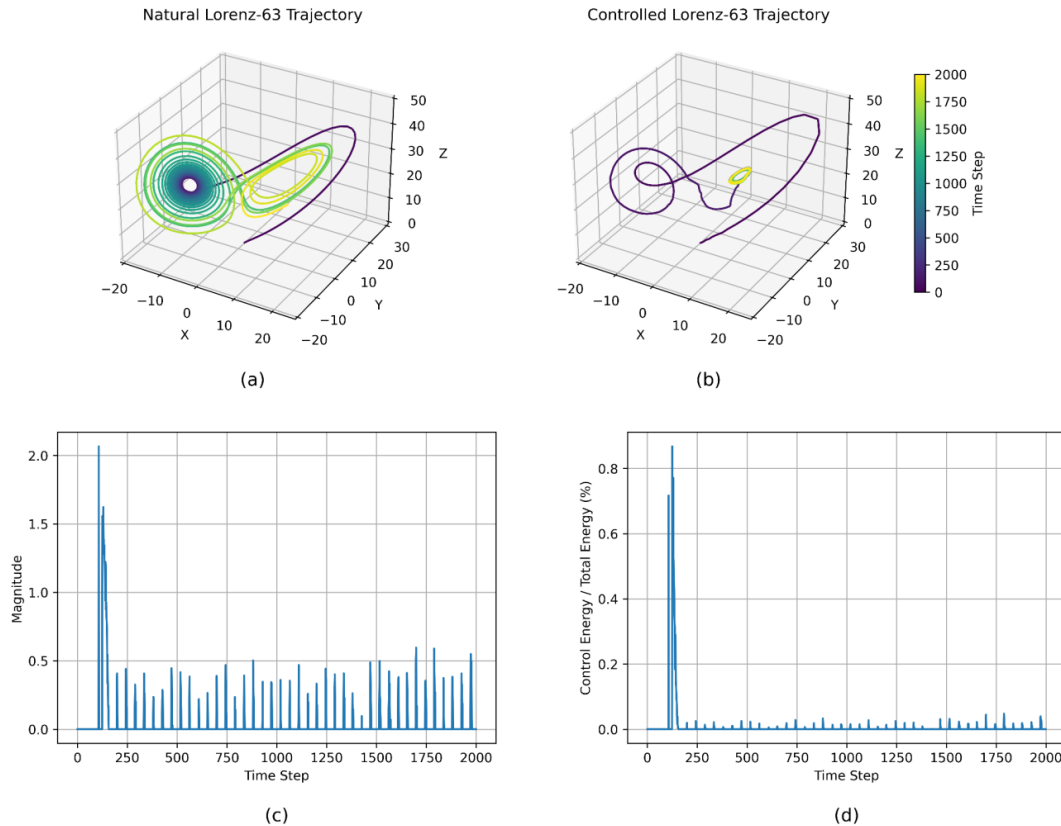


Figure 3: Comparison of natural (a) and controlled (b) L63 trajectories under an unstable initial condition. (c) shows the magnitude of perturbations applied at each step, and (d) displays the ratio of control energy to total system energy over time.

3.3 LLE Thresholds Trade-off Between Timeliness and Efficiency

Tuning the LLE threshold allows for better balance between early intervention and total energy cost. By varying the threshold used to trigger control, we assess the sensitivity of the control strategy to instability detection (Supporting Information S4). High thresholds delay intervention, allowing the system to evolve further into chaotic regimes before correction. While this reduces the number of control actions, it also results in higher energy usage due to stronger perturbations being required. In contrast, very low thresholds (e.g., -1.0) lead to frequent interventions. Across tested values, thresholds between -0.5 and 0.0 provided the best balance, stabilizing the system efficiently while minimizing energy costs. These results suggest that optimizing the LLE threshold is useful for deploying energy-efficient control strategies in chaotic systems.



3.4 Control of Eddies in L84

To determine an appropriate state space for specifying control of the eddy energy in the L84 model, we analyse the relationship between eddy magnitude, represented by $|Y|+|Z|$, and LLE value over 10,000 time steps. As shown in Supporting Information S5 and S6, both quantities exhibit strong temporal fluctuations, with higher LLE values generally coinciding with peaks in $|Y|+|Z|$. This reflects the fact that the system becomes more unstable and chaotic when eddy amplitudes grow large, consistent with physical intuition. We select the 90th percentile of $|Y|+|Z|$ as a threshold, which corresponds to an LLE value of approximately 2.4. Recall that in this case our goal is to act in the short term to suppress eddy growth to very high values, unlike the L63 case where the goal was to exercise continuous time control over the system state.

To assess the effectiveness of the control strategy applied to the L84 model, we compare the natural and controlled system trajectories (Figure 4). The natural trajectory exhibits strong variability and excursions beyond a threshold radius $|Y|+|Z|>2.4$, indicating very active eddies. In contrast, the controlled trajectory remains well-contained within the inner region of the attractor. Supporting Information S7 quantifies the control effort, showing that the control energy remains below 2% of the total system energy for the majority of the simulation, with only occasional peaks when the system is at risk of transitioning to unstable behaviour. These results indicate that the applied control strategy can limit the extreme eddies in the L84 system.

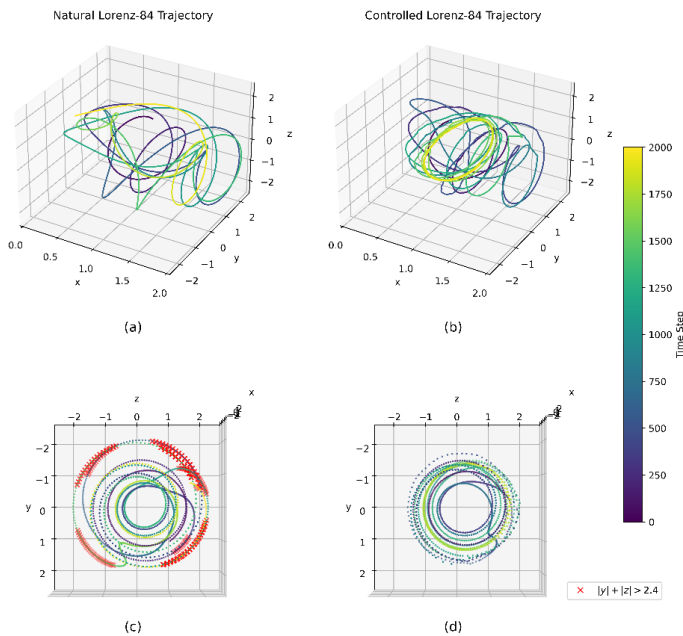


Figure 4: Coloured trajectory plots of L84 under natural (a, c) and controlled (b, d) conditions from two different viewing angles. Red dots in (c) and (d) indicate time steps where the combined eddy amplitude satisfies $|Y|+|Z|>2.4$



3.5 Computational Aspects of the Control Method

Each optimization step completes in under 0.1 seconds, enabling potential real-time or online applications. The selective control strategy relies on solving a constrained optimization problem at each intervention step using the SLSQP algorithm. Across 2000 time steps, the average runtime per optimization was approximately 0.09 seconds. For the L63 simulation, this resulted in a total runtime of ~80 seconds. In the L84 case, runtime increased to ~25 seconds due to the rare extreme scenario events. All simulations were executed in Python 3.11.3 on a system with an i386 architecture, 2 physical cores (4 logical), using a single-threaded configuration. These results indicate that the control method is computationally feasible for the idealized models, and could be further accelerated through parallelization or compiled implementations.

4 Discussion and Conclusions

Our intent was to explore whether a practically motivated approach to simulation and adaptive control could be effective for two target idealized atmospheric models, with slightly different goals. We were able to demonstrate computational and operational feasibility and explore conditions that are challenging and sensitivity to parameter choices. Previous control approaches for chaotic systems, such as Sliding Mode Control (SMC), Time-delayed Feedback (TDF), and reinforcement learning (RL), offer useful frameworks but face limitations in practical weather applications. SMC is known for robustness but induces chattering, making it unsuitable for smooth, energy-efficient interventions (Yau and Yan, 2004; Yang et al., 2002; Vaidyanathan and Sampath, 2011). TDF control avoids full model dependence but relies heavily on past states, which is problematic in high-dimensional, chaotic systems like the atmosphere (Pyragas and Pyragas, 2006; Postlethwaite and Silber, 2007; Purewal et al., 2016). RL offers flexibility but often demands prohibitive computational resources (Ding and Lei, 2023). Japanese researchers are currently working with Japan's Moonshot 8 project aiming to achieve controlling and modifying weather by 2050 (Miyoshi and Sun, 2022; Nakazawa, 2024). Their approach applies Control Simulation Experiments (CSE) and Model Predictive Control (MPC) to constrain L63 dynamics to one wing of the attractor, emphasizing data assimilation to select stable ensemble trajectories for potential real-world implementation.

In contrast, we propose a predictive model-based strategy that can forecast future trajectories directly, potentially reducing computational demands. we target model-defined extreme states (regime shifts in L63 and large eddies in L84) rather than generic trajectory stabilization, linking the control problem to conceptually relevant meteorological phenomena. We explicitly incorporate noise to account for uncertainty in both model dynamics and observations. This allows us to evaluate control robustness under realistic variability. Instead of addressing energy efficiency and selective control activation as separate objectives, our method integrates both: it activates control only when instability is detected, while simultaneously minimizing energy use. The resulting framework operates efficiently, responds flexibly to emerging instability, and aligns with the philosophy of "Weather Jiu-Jitsu": subtly redirecting rather than resisting chaotic dynamics.



To extend this concept to operational weather systems, we will integrate our control framework with recent advances in data-driven forecasting and real-time decision-making. Our ongoing work focuses on combining deep learning foundation models, such as Chronos, Aurora, Prithvi wXc and GenCast, extending the approach demonstrated here to a dramatically higher dimensional space. While the conceptual logic remains the same, the decision process must now address where and when to intervene, targeting specific spatio-temporal attributes of concern. Of course, these are still thought experiments, motivated by the very high potential value of disaster reduction, and one also needs to identify practical mechanisms for creating the perturbations. Some ideas in that regard are discussed in (Huang et al., 2025). These are challenging problems and we invite collaborations on all aspects of developing the ideas.

5 Code/Data availability

No new data were used in this study. All results are based on a theoretical model described in the manuscript. Therefore, no data or software are archived. All code can be provided by the corresponding authors upon request.

6 Author contribution

Moyan Liu, Qin Huang, and Upmanu Lall jointly conceived the study and designed the experiments. All authors contributed to developing the control framework, implementing the model code, and performing the simulations. The manuscript was prepared collaboratively, with equal contributions from all authors.

7 Competing interests

The authors declare that they have no conflict of interest.



References

- Aemisegger, F., Vogel, R., Graf, P., Dahinden, F., Villiger, L., Jansen, F., Bony, S., Stevens, B., and Wernli, H.: How
 315 Rossby wave breaking modulates the water cycle in the North Atlantic trade wind region, *Weather and Climate
 Dynamics*, 2, 281-309, 10.5194/wcd-2-281-2021, 2021.
- Aurell, E., Boffetta, G., Crisanti, A., Paladin, G., and Vulpiani, A.: Predictability in the large: an extension of the
 concept of Lyapunov exponent, *J. Phys. A: Math. Gen.*, 30, 1-26, 10.1088/0305-4470/30/1/003, 1997.
- Boccaletti, S., Farini, A., Kostelich, E. J., and Arecchi, F. T.: Adaptive targeting of chaos, *Phys. Rev. E*, 55, R4845-
 320 R4848, 10.1103/PhysRevE.55.R4845, 1997.
- Boltt, E.: Targeting Control of Chaotic Systems,
- Broer, H., Simó, C., and Vitolo, R.: Bifurcations and strange attractors in the Lorenz-84 climate model with seasonal
 forcing, *Nonlinearity*, 15, 1205, 10.1088/0951-7715/15/4/312, 2002.
- Ding, J. and Lei, Y.: Control of chaos with time-delayed feedback based on deep reinforcement learning, *Physica D:
 325 Nonlinear Phenomena*, 451, 133767, 10.1016/j.physd.2023.133767, 2023.
- Eckhardt, B. and Yao, D.: Local Lyapunov exponents in chaotic systems, *Physica D: Nonlinear Phenomena*, 65, 100-
 108, 10.1016/0167-2789(93)90007-N, 1993.
- Faranda, D., Sato, Y., Messori, G., Moloney, N. R., and Yiou, P.: Minimal dynamical systems model of the Northern
 Hemisphere jet stream via embedding of climate data, *Earth Syst. Dynam.*, 10, 555-567, 10.5194/esd-10-555-2019,
 330 2019.
- Freire, J. G., Bonatto, C., DaCamara, C. C., and Gallas, J. A. C.: Multistability, phase diagrams, and intransitivity in
 the Lorenz-84 low-order atmospheric circulation model, *Chaos: An Interdisciplinary Journal of Nonlinear Science*,
 18, 033121, 10.1063/1.2953589, 2008.
- Glasner, E. and Weiss, B.: Sensitive dependence on initial conditions, *Nonlinearity*, 6, 1067, 10.1088/0951-
 335 7715/6/6/014, 1993.
- Grebogi, C. and Lai, Y.-C.: Controlling chaotic dynamical systems, *Systems & Control Letters*, 31, 307-312,
 10.1016/S0167-6911(97)00046-7, 1997.
- Guégan, D. and Leroux, J.: Local Lyapunov Exponents: A New Way to Predict Chaotic Systems, in: *Topics on Chaotic
 Systems, Topics on Chaotic Systems - Selected Papers from CHAOS 2008 International Conference*, 2009/05//, 158-
 340 165, 10.1142/9789814271349_0018,
- Han, J. and Singh, V. P.: Impacts of Rossby Wave Packets and Atmospheric Rivers on Meteorological Drought in the
 Continental United States, *Water Resources Research*, 57, e2021WR029966, 10.1029/2021WR029966, 2021.
- Hoffman, R. N.: Controlling The Global Weather, *Bull. Amer. Meteor. Soc.*, 83, 241-248, 10.1175/1520-
 0477(2002)083<0241:CTGW>2.3.CO;2, 2002.
- 345 Huang, Q., Liu, M., and Lall, U.: Weather Jiu-Jitsu: Climate Adaptation for the 21st Century, 2025.
- Hwang, J. and Lall, U.: Increasing dam failure risk in the USA due to compound rainfall clusters as climate changes,
npj Nat. Hazards, 1, 27, 10.1038/s44304-024-00027-6, 2024.
- Karamperidou, C., Cioffi, F., and Lall, U.: Surface Temperature Gradients as Diagnostic Indicators of Midlatitude
 Circulation Dynamics, 10.1175/JCLI-D-11-00067.1, 2012.



- 350 Kawasaki, F. and Kotsuki, S.: Leading the Lorenz 63 system toward the prescribed regime by model predictive control coupled with data assimilation, *Nonlinear Processes in Geophysics*, 31, 319-333, 10.5194/npg-31-319-2024, 2024.
- Kim, J.-H., Nam, S.-H., Kim, M.-K., Serrano-Notivol, R., and Tejedor, E.: The 2022 record-high heat waves over southwestern Europe and their underlying mechanism, *Weather and Climate Extremes*, 46, 100729, 10.1016/j.wace.2024.100729, 2024.
- 355 Kraft, D.: A software package for sequential quadratic programming, DLR German Aerospace Center — Institute for Flight Mechanics, Köln, Germany, 1988.
- Lapeyre, G.: Characterization of finite-time Lyapunov exponents and vectors in two-dimensional turbulence, *Chaos: An Interdisciplinary Journal of Nonlinear Science*, 12, 688-698, 10.1063/1.1499395, 2002.
- Liapounoff, A.: Problème général de la stabilité du mouvement, *Annales de la Faculté des sciences de l'Université de Toulouse pour les sciences mathématiques et les sciences physiques*, 9, 203-474, 1907.
- 360 Lorenz, E. N.: Deterministic Nonperiodic Flow, 1963.
- Lorenz, E. N.: Irregularity: a fundamental property of the atmosphere, *Tellus A: Dynamic Meteorology and Oceanography*, 36, 98, 10.3402/tellusa.v36i2.11473, 1984.
- Lorenz, E. N.: Can chaos and intransitivity lead to interannual variability?, *Tellus A*, 42, 378-389, <https://doi.org/10.1034/j.1600-0870.1990.t01-2-00005.x>, 1990.
- 365 MacMynowski, D. G.: Controlling chaos in El Niño, in: *Proceedings of the 2010 American Control Conference*, the 2010 American Control Conference, 2010/06//, 4090-4094, 10.1109/ACC.2010.5530629,
- Madonna, E., Li, C., Grams, C. M., and Woollings, T.: The link between eddy-driven jet variability and weather regimes in the North Atlantic-European sector, *Quart J Royal Meteor Soc*, 143, 2960-2972, 10.1002/qj.3155, 2017.
- 370 Mario, E., Raffaele, L., Onofrio, C., Maria, C.-S. J., Valentina, B., Vincenzo, G., Shao, C., and Giovanni, S.: Coupling heat wave and wildfire occurrence across multiple ecoregions within a Eurasia longitudinal gradient, *Science of The Total Environment*, 912, 169269, 10.1016/j.scitotenv.2023.169269, 2024.
- Mitsui, T., Kotsuki, S., Fujiwara, N., Okazaki, A., and Tokuda, K.: Bottom-up approach for mitigating extreme events under limited intervention options: a case study with Lorenz 96, 10.5194/egusphere-2025-987, 2025.
- 375 Miyoshi, T. and Sun, Q.: Control simulation experiment with Lorenz's butterfly attractor, *Nonlinear Processes in Geophysics*, 29, 133-139, 10.5194/npg-29-133-2022, 2022.
- Nabizadeh, E., Hassanzadeh, P., Yang, D., and Barnes, E. A.: Size of the Atmospheric Blocking Events: Scaling Law and Response to Climate Change, *Geophysical Research Letters*, 46, 13488-13499, 10.1029/2019GL084863, 2019.
- Nagai, R., Bai, Y., Ogura, M., Kotsuki, S., and Wakamiya, N.: Evaluation of Effectiveness of Intervention Strategy in Control Simulation Experiment through Comparison with Model Predictive Control, 10.5194/npg-2024-26, 2024.
- 380 Nakazawa, T. M., T.; Sakajo, T.; Takatama, K.: An overview of Japan's Moonshot Goal 8 R&D program for controlling and modifying the weather by 2050, *EGU General Assembly 2024*, Vienna, Austria, 14–19 April 2024, <https://doi.org/10.5194/egusphere-egu24-13655>, 2024.
- Newman, M., Kiladis, G. N., Weickmann, K. M., Ralph, F. M., and Sardeshmukh, P. D.: Relative Contributions of Synoptic and Low-Frequency Eddies to Time-Mean Atmospheric Moisture Transport, Including the Role of Atmospheric Rivers, *Journal of Climate*, 25, 7341-7361, <https://doi.org/10.1175/JCLI-D-11-00665.1>, 2012.
- 385



- Ogorzałek, M. J.: Chaos control: How to avoid chaos or take advantage of it, *Journal of the Franklin Institute*, 331, 681-704, 10.1016/0016-0032(94)90086-8, 1994.
- Ott, E., Grebogi, C., and Yorke, J. A.: Controlling chaos, *Phys. Rev. Lett.*, 64, 1196-1199, 10.1103/PhysRevLett.64.1196, 1990.
- Ouyang, M., Tokuda, K., and Kotsuki, S.: Reducing manipulations in a control simulation experiment based on instability vectors with the Lorenz-63 model, *Nonlinear Processes in Geophysics*, 30, 183-193, 10.5194/npg-30-183-2023, 2023.
- Palmer, T. N.: Predictability of weather and climate: from theory to practice, in: *Predictability of Weather and Climate*, 1 ed., edited by: Palmer, T., and Hagedorn, R., Cambridge University Press, 1-29, 2006.
- Postlethwaite, C. M. and Silber, M.: Stabilizing unstable periodic orbits in the Lorenz equations using time-delayed feedback control, *Phys. Rev. E*, 76, 056214, 10.1103/PhysRevE.76.056214, 2007.
- Purewal, A. S., Krauskopf, B., and Postlethwaite, C. M.: Global Effects of Time-Delayed Feedback Control Applied to the Lorenz System, in: *Control of Self-Organizing Nonlinear Systems*, edited by: Schöll, E., Klapp, S. H. L., and Hövel, P., Springer International Publishing, Cham, 81-103, 2016.
- Pyragas, V. and Pyragas, K.: Delayed feedback control of the Lorenz system: An analytical treatment at a subcritical Hopf bifurcation, *Phys. Rev. E*, 73, 036215, 10.1103/PhysRevE.73.036215, 2006.
- Robinson, A., Lehmann, J., Barriopedro, D., Rahmstorf, S., and Coumou, D.: Increasing heat and rainfall extremes now far outside the historical climate, *npj Climate and Atmospheric Science*, 4, 45, 10.1038/s41612-021-00202-w, 2021.
- Saiki, Y. and Yorke, J. A.: Can the Flap of a Butterfly's Wings Shift a Tornado into Texas—Without Chaos?, *Atmosphere*, 14, 821, 10.3390/atmos14050821, 2023.
- Saltzman, B.: EQUATIONS GOVERNING THE ENERGETICS OF THE LARGER SCALES OF ATMOSPHERIC TURBULENCE IN THE DOMAIN OF WAVE NUMBER, *Journal of Atmospheric Sciences*, 14, 513-523, [https://doi.org/10.1175/1520-0469\(1957\)014<0513:EGTEOT>2.0.CO;2](https://doi.org/10.1175/1520-0469(1957)014<0513:EGTEOT>2.0.CO;2), 1957.
- Saltzman, B.: On the Maintenance of the Large-Scale Quasi-Permanent Disturbances in the Atmosphere, *Tellus A: Dynamic Meteorology and Oceanography*, 11, 425-431, 10.3402/tellusa.v11i4.9329, 1959.
- Shen, B.-W., Pielke, R. A., Zeng, X., Baik, J.-J., Faghih-Naini, S., Cui, J., and Atlas, R.: Is Weather Chaotic?: Coexistence of Chaos and Order within a Generalized Lorenz Model, 10.1175/BAMS-D-19-0165.1, 2021.
- Sugiyama, M., Asayama, S., Kosugi, T., Ishii, A., and Watanabe, S.: Public attitude toward solar radiation modification: results of a two-scenario online survey on perception in four Asia-Pacific countries, *Sustain Sci*, 20, 423-438, 10.1007/s11625-024-01520-7, 2025.
- Vaidyanathan, S. and Sampath, S.: *Global Chaos Synchronization of Hyperchaotic Lorenz Systems by Sliding Mode Control*, Berlin, Heidelberg, 156-164,
- Van Veen, L.: Baroclinic Flow and the Lorenz-84 Model, *Int. J. Bifurcation Chaos*, 13, 2117-2139, 10.1142/S0218127403007904, 2003.
- Wolf, A., Swift, J. B., Swinney, H. L., and Vastano, J. A.: Determining Lyapunov exponents from a time series, *Physica D: Nonlinear Phenomena*, 16, 285-317, 10.1016/0167-2789(85)90011-9, 1985.



- Yang, S. K., Chen, C. L., and Yau, H. T.: Control of chaos in Lorenz system, *Chaos, solitons and fractals*, 13, 767-780, 10.1016/S0960-0779(01)00052-2, 2002.
- Yau, H.-T. and Yan, J.-J.: Design of sliding mode controller for Lorenz chaotic system with nonlinear input, *Chaos, Solitons & Fractals*, 19, 891-898, 10.1016/S0960-0779(03)00255-8, 2004.
- Yeh, E. T.: Global Geographies of Weather Modification in an Era of Climate Change, *Annals of the American Association of Geographers*, 115, 949-967, 10.1080/24694452.2025.2450200, 2025.
- 430 Yu, X.: Controlling Lorenz chaos, *International Journal of Systems Science*, 27, 355-359, 10.1080/00207729608929224, 1996.
- Zhao, Y.: CCUS: A Panacea or a Placebo in the fight against climate change?, *Green Energy & Environment*, 10, 239-243, 10.1016/j.gee.2024.10.001, 2025.
- Zhu, Y. and Newell, R. E.: A Proposed Algorithm for Moisture Fluxes from Atmospheric Rivers, *Monthly Weather*
- 435 Review, 126, 725-735, [https://doi.org/10.1175/1520-0493\(1998\)126<0725:APAFMF>2.0.CO;2](https://doi.org/10.1175/1520-0493(1998)126<0725:APAFMF>2.0.CO;2), 1998.